Journal of Magnetic Resonance **144,** 53–57 (2000)
doi:10.1006/jmre.2000.2052, available online at http://www.idealibrary.com on IDEAL®

# Remote Tuning of NMR Probe Circuits

Vikram D. Kodibagkar and Mark S. Conradi

*Department of Physics—1105, Washington University, St. Louis, Missouri 63130-4899*

Received August 18, 1999; revised January 25, 2000

**There are many circumstances in which the probe tuning adjustments cannot be located near the rf NMR coil. These may occur in high-temperature NMR, low-temperature NMR, and in the use of magnets with small diameter access bores. We address here circuitry for connecting a fixed-tuned probe circuit by a transmission line to a remotely located tuning network. In particular, the bandwidth over which the probe may be remotely tuned while keeping the losses in the transmission line acceptably low is considered. The results show that for all resonant circuit geometries (series, parallel, series–parallel), overcoupling of the line to the tuned circuit is key to obtaining a large tuning bandwidth. At equivalent extents of overcoupling, all resonant circuit geometries have nearly equal remote tuning bandwidths. Particularly for the case of low-loss transmission line, the tuning bandwidth can be many times the tuned circuit's bandwidth,** $f_o/Q$. 

*Key Words:* **remote tuning; probe.**

## I. INTRODUCTION

The NMR probe tuned-circuit serves to couple the spin magnetization to the transmitting and receiving amplifiers. Thus, the probe circuit determines the NMR performance, both the power required to generate a given rf field $H_1$ and the signal-to-noise available in the receiver from a given precessing spin magnetization. It is generally recognized that optimum probe performance is obtained with all of the tuning and matching components located near the NMR coil, so that the only loss in the circuit is the unavoidable loss of the coil itself (*1, 2*). We take as given that the rf coil has already been optimized (*3*).

However, it is often difficult to locate the tuning-matching components close to the coil. In particular, the *adjustable* components (e.g., variable tuning capacitors) may be too bulky or may not be compatible with the sample environment (particularly high or low temperatures). Fixed tuning of the probe is generally unacceptable, because temperature excursions, etc., will change the resonant frequency by more than the probe bandwidth of $f_o/Q$. There are many clever solutions to this problem, including the use of evacuated and small tuning capacitors (*4, 5*), capacitors that tune by motion of a dielectric with no sliding contacts (*6, 7*), inductive tuning (*8, 9*), and more. We note that some of these solutions require careful mechanical designs.

A less elegant but easily implemented approach is to approximately tune and match the NMR coil with fixed components located near the coil. Remote fine-tuning and matching is required to compensate for frequency shifts of the probe circuit (e.g., due to temperature changes). Remote tuning and matching is accomplished with variable reactances on the distant end of a transmission line (*10, 11*). This approach makes use of the transmission line which is present in any event (i.e., to connect the spectrometer to the probe). The remote components may be conveniently located at room temperature and may be physically large so as to be nearly loss-free, with high voltage and power ratings. However, to the extent that standing waves are present on the line, there may be substantial power dissipation (loss) on the line (*12–14*), reducing the NMR performance on both transmit and receive. We stress that the advantage of remote tuning and matching is design convenience, particularly with NMR coils at very low or very high temperatures or where space is not available, as in narrow bore magnets or narrow cryostats (*5*) or in diamond anvil cell NMR (*15*). There is no performance advantage to remote tuning and matching; at best, such a design can hope only to equal the performance of a locally tuned and matched coil.

We consider here circuitry in which the probe-tuned circuit is connected by a transmission line to remote tuning elements. In particular, we address the *tuning bandwidth*, the frequency extent over which the circuit may be remotely tuned while maintaining acceptably low losses in the transmission line. While transmission line probes have been described before (*16–18*) and remote tuning has been analyzed (*10, 11*) and employed in a sophisticated multiple-frequency probe (*19*), the issue of tuning bandwidth has not been systematically addressed before. The present results are expected to be of most relevance to NMR at extreme temperatures (which result in substantial tuning changes), diamond anvil cell NMR (*15*) (where distortions of the gasket will change the tuning), and with very broad NMR lines (e.g., to be able to tune across quadrupole-broadened resonances in solids).

## II. RESULTS AND DISCUSSION

We consider a tuned circuit of any of the geometries of Fig. 1, connected to the external world through a transmission line.



1090-7807/00 $35.00

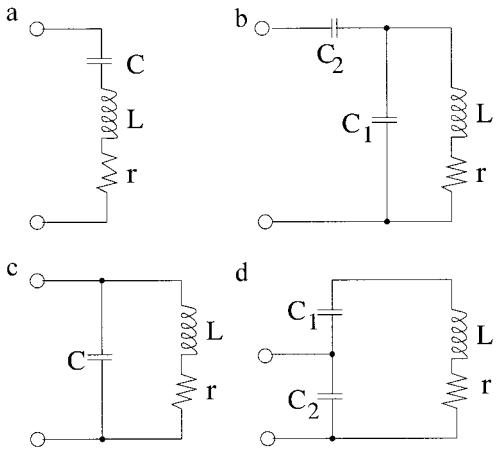


**FIG. 1.** Tuned circuit geometries for NMR probe circuits: (a) series resonant, (b) capacitive top-feed, where the current division ratio is $C_2/(C_1 + C_2)$, (c) parallel resonant, and (d) capacitive voltage divider. In all cases, $r$ represents the NMR coil L's losses, with $r = \omega_o L/Q$.

Such a system could be used with 100% efficiency at any frequency (near or far from the resonance frequency), provided the line were loss-free. Here we assume that any complex impedance can be transformed to the spectrometer's impedance (e.g., 50 ohms real) using large, loss-free components at the room-temperature end of the transmission line. Throughout the present analysis, this assumption is used. We note that wide-range impedance transforming networks are widely used in radio to transform the impedance of an arbitrary-length antenna to match the receiver and/or transmitter.

The crucial issue in remotely tuned probe circuits is the *dissipation* on the transmission line, which is never loss-free. If the tuned circuit impedance is not equal to $R_o$, the characteristic impedance of the line (assumed to be real), a standing wave will exist on the line and decrease the efficiency for both receiving and transmitting. For a probe circuit with complex impedance $Z$, the reflection coefficient $\rho$ at the transmission line-tuned circuit connection is (*12–14*)

$$\rho = |(Z - R_o)/(Z + R_o)|. \qquad [1]$$

For $\rho > 0$, the line will carry both forward and reflected waves.

The power efficiency $\eta$ of the transmission line is defined by the ratio of the power delivered to the load (tuned circuit) to the input power (from the spectrometer's transmitter). We assume the transmission line is either an integer number of half-wavelengths long or much longer than $\lambda/2$. In either case, the cross-terms between forward and reflected waves are zero or negligible in calculating the power dissipated by the line. The efficiency $\eta$ becomes (*12–14*)

$$\eta = \frac{e^{2\alpha L}(1 - \rho^2)}{e^{4\alpha L} - \rho^2}. \qquad [2]$$

Here $\alpha L$ describes the exponential voltage attenuation along the line when matched (i.e., $\exp(-\alpha L)$; $\alpha$ is the attenuation per length and $L$ is the line length). Thus, the attenuation of the line (when matched) in dB is $20\alpha L(0.4343)$. As $\rho$ grows toward unity in Eq. [2], the efficiency will decrease. The decrease in efficiency with increasing reflection coefficient and standing wave ratio has been explained qualitatively (*16*).

Four geometries of tuned circuit will be addressed, as presented in Fig. 1. For the series resonant circuit (Fig. 1a), the impedance at resonance is $R_{\text{res}} = r = \omega_o L/Q$. For practical component values and high $Q$, this impedance is often impractically small. Thus the capacitive top-feed configuration (Fig. 1b) is widely used. Here, the circulating current is divided between $C_1$ and $C_2$. This circuit may be viewed as a series resonance with impedance step-up. The current division ratio is $C_2/(C_1 + C_2)$, so the (real) impedance at resonance is increased by the inverse square of this ratio:

$$R_{\text{res}} = (\omega_o L/Q)[(C_1 + C_2)/C_2]^2. \qquad [3]$$

For the resonance condition, $C_1$ and $C_2$ are effectively in parallel: $\omega_o^2 L(C_1 + C_2) = 1$. We note that the above equations are extremely good approximations for this circuit, for $Q \gg 1$ and $1/(\omega_o C_2) \gg R_{\text{res}}$ (meaning the current division ratio must satisfy $[C_2/(C_1 + C_2)]Q \gg 1$, as nearly always occurs for practical values).

For the parallel-tuned circuit of Fig. 1c, the real impedance at resonance is $R_{\text{res}} = Q\omega_o L = (\omega_o L)^2/r$. For high $Q$ and practical component values, this resistance may be impractically large. Thus the capacitive voltage divider configuration (Fig. 1d) may be used. Here the coil voltage is divided by $C/C_2$, where $C$ is the series combination of $C_1$ and $C_2$ ($C^{-1} = C_1^{-1} + C_2^{-1}$). Thus the circuit may be regarded as a parallel resonance with impedance step-down. The resistance at resonance is

$$R_{\text{res}} = (Q\omega_o L)(C/C_2)^2. \qquad [4]$$

The resonance condition is $\omega_o^2 LC = 1$. Again, these equations are very good approximations for $Q \gg 1$ and $1/\omega_o C_2 \ll R_{\text{res}}$ (meaning the voltage division ratio must obey $(C/C_2)Q \gg 1$, nearly always true with practical values).

A key concept in understanding the tuning bandwidth is the extent of overcoupling ($EOC$) of the transmission line to the tuned circuit. For a transmission line of characteristic (real) impedance $R_o$, we define the $EOC$ as $EOC = R_o/R_{\text{res}}$ for the series resonant geometries of Figs. 1a and 1b. For the parallel resonant arrangements of Figs. 1c and 1d, $EOC = R_{\text{res}}/R_o$. Thus, for the circuits of Figs. 1a, 1b, 1c, and 1d, respectively:

$$EOC = R_o/r, \qquad [5a]$$

$$EOC = R_o/[r(C_1 + C_2)^2/C_2^2], \qquad [5b]$$

$$EOC = Q\omega_o L/R_o, \quad [5c]$$

$$EOC = (Q\omega_o LC^2/C_2^2)/R_o. \quad [5d]$$

Calculations were performed on a computer, giving the impedance of the tuned circuits of Fig. 1 as a function of frequency. The reflection coefficient $\rho$ and the efficiency $\eta$ were computed using Eqs. [1] and [2]. The tuned circuit parameters were $L = 0.5$ $\mu$H, $\omega_o = 100 \times 10^6$ rad/s, $Q = 100$, and $R_o = 50$ ohms, unless stated otherwise. Compared to calculations with dimensionless variables, use of the values given allows one to more readily identify physically unrealistic parameters.

The importance of the matched loss $\alpha L$ of the transmission line is demonstrated in Fig. 2. There the efficiency $\eta$ is presented for $\alpha L = 0.05$ (top) and $\alpha L = 0.005$ (bottom), for parallel tuned circuits (Fig. 1c) with several values of the extent of overcoupling of the line to the circuit, as in Eq. [5c]. The upper case corresponds to a 1.5 m length of ordinary RG-58A/U at 250 MHz, while the lower case corresponds to very low-loss line made from large copper tubing (about 2 cm diameter of outer conductor).

From Fig. 2, it is evident that the bandwidth over which acceptable performance (e.g., $\eta > 0.5$) may be obtained is much larger than the 1% bandwidth of the $L$–$C$ circuit itself ($Q = 100$). This is particularly true for the low-loss line, where an efficiency $\eta > 0.8$ can be obtained across a $\pm 10\%$ frequency range, with an overcoupling of $EOC = 16$. The "coil-only" case uses a coil of $Q = 100$ with $\omega_o L$ chosen equal to $R_o$ (the optimum value, as shown in Ref. (*2*)). The efficiencies at the center frequency are only 0.1 and 0.5 for the two choices of transmission line, though the performance is virtually flat as a function of frequency. We note that one successful multiple-resonance design uses no tuning of the rf coil, with extremely low-loss line (*17*).

Ultimately, the design goal for a probe circuit is good power efficiency. But because efficiency depends upon the matched-line loss $\alpha L$ as well as the circuit parameters, all further results here will be presented in terms of the reflection coefficient $\rho$ of Eq. [1]. The efficiency may then be computed by means of Eq. [2].

Results are presented in Fig. 3 for capacitively top-fed tuned circuits of Fig. 1b. We note the logarithmic scale at left, with corresponding values of $\rho$ at right. Several values of (unloaded) $Q$ are used, with the circuit adjusted to exactly match the line at the center frequency (i.e., the current division ratio $C_2/(C_1 + C_2)$ is selected so that $R_{\text{res}}$ of Eq. [3] is equal to the characteristic impedance of the line, $R_o$). In Fig. 3 it is evident that the bandwidth for a given maximum value of $\rho$ is proportional to $1/Q$. Thus, obtaining a sufficient tuning bandwidth will generally be an issue only for high values of the unloaded $Q$.

The effect of the extent of overcoupling on the tuning bandwidth is presented in Fig. 4. All circuits are the geometry

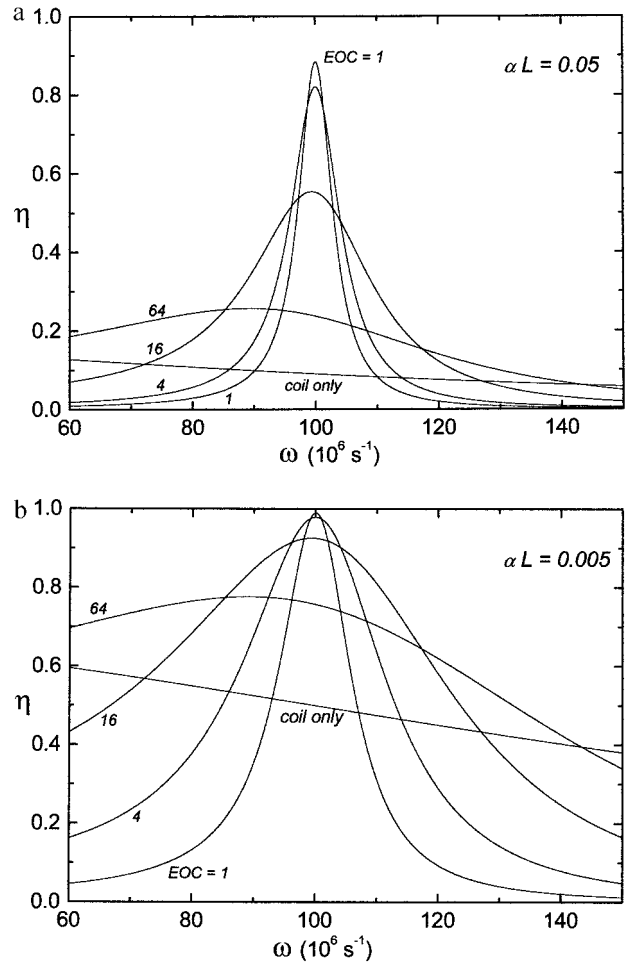


**FIG. 2.** Transmission line power efficiency $\eta$ for $R_o = 50$ ohm line with $\alpha L = 0.05$ (0.43 dB matched loss) at top and with $\alpha L = 0.005$ (0.043 dB matched loss) at bottom. The probe circuit is a parallel tuned circuit with unloaded $Q = 100$ and center frequency $\omega_o = 100 \times 10^6$ s$^{-1}$. Results are shown for different $L/C$ ratios, corresponding to various extents of overcoupling ($EOC$) of the line to the tuned circuit, as shown. Shown for comparison is an untuned coil, with $\omega_o L$ chosen to equal $R_o$. The tuning bandwidths become larger with greater $EOC$ and with smaller matched line loss. Especially for low-loss line (bottom), the tuning bandwidth may greatly exceed the natural bandwidth of the $L$–$C$ circuit, $f_o/Q$.

of Fig. 1b with $Q = 100$, with the current division ratio varied to yield $EOC$ values from 0.25 (undercoupled) to 32 (severely overcoupled to the line). Clearly, the undercoupled circuit's performance is inferior (larger $\rho$) to the optimally coupled circuit ($EOC = 1$), at all frequencies. At the center frequency, the $EOC = 1$ case has the best performance, of course. But if one desires a broader frequency range, the overcoupled circuits ($EOC > 1$) are superior, at the expense of somewhat poorer performance at the center frequency (higher reflection coefficient and resultingly decreased power efficiency). Thus, it is important to design for only the *required* tuning bandwidth.

The circuit of Fig. 1b may be conveniently regarded as an impedance stepped-up series resonance, but it is more compli-

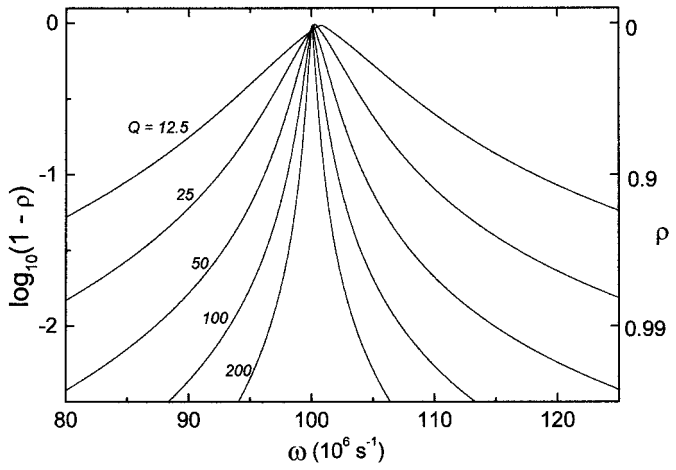


**FIG. 3.** Reflection coefficient $\rho$ versus operating frequency for tuned circuits of capacitive top-feed geometry of Fig. 1b, for several values of unloaded $Q$. In each case, the coupling capacitor is adjusted to yield a perfect match to the transmission line at the center frequency. The tuning bandwidth for a given maximum allowable reflection coefficient varies as $1/Q$, showing that the tuning bandwidth scales with the circuit's natural width, $f_o/Q$. The logarithmic scale at left corresponds to the values of $\rho$ at right.

cated. For example, in addition to the series resonance (impedance minimum) at $\omega_o^2 L(C_1 + C_2) = 1$, there is a parallel resonance (maximum impedance) at $\omega^2 LC_1 = 1$. Similarly for the capacitive voltage divider of Fig. 1d, the parallel resonance at $\omega_o^2 LC = 1$ (with $C$ the series combination of $C_1$ and $C_2$) is accompanied by a series resonance at a lower frequency, $\omega^2 LC_1 = 1$.

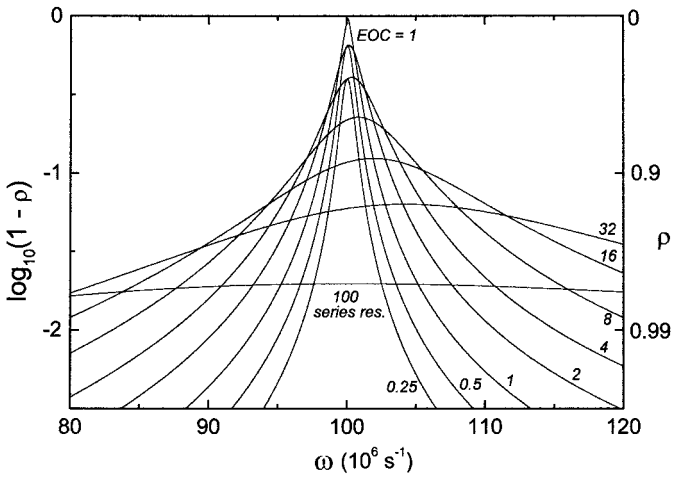


**FIG. 4.** Reflection coefficient $\rho$ as a function of operating frequency. The $L$–$C$ circuits are all capacitive top-feed geometry of Fig. 1b with $Q = 100$, and with the coupling adjusted to yield the several values of $EOC$ listed (extends of overcoupling of the line to the $L$–$C$ circuit). The cases shown span from undercoupled ($EOC < 1$) to very overcoupled ($EOC \gg 1$); a simple series resonant coil ($\omega_o L = R_o$ and $Q = 100$) is presented for comparison. For a desired bandwidth across which the reflection coefficient must be maintained below some maximum value, there is an optimum value of $EOC$.

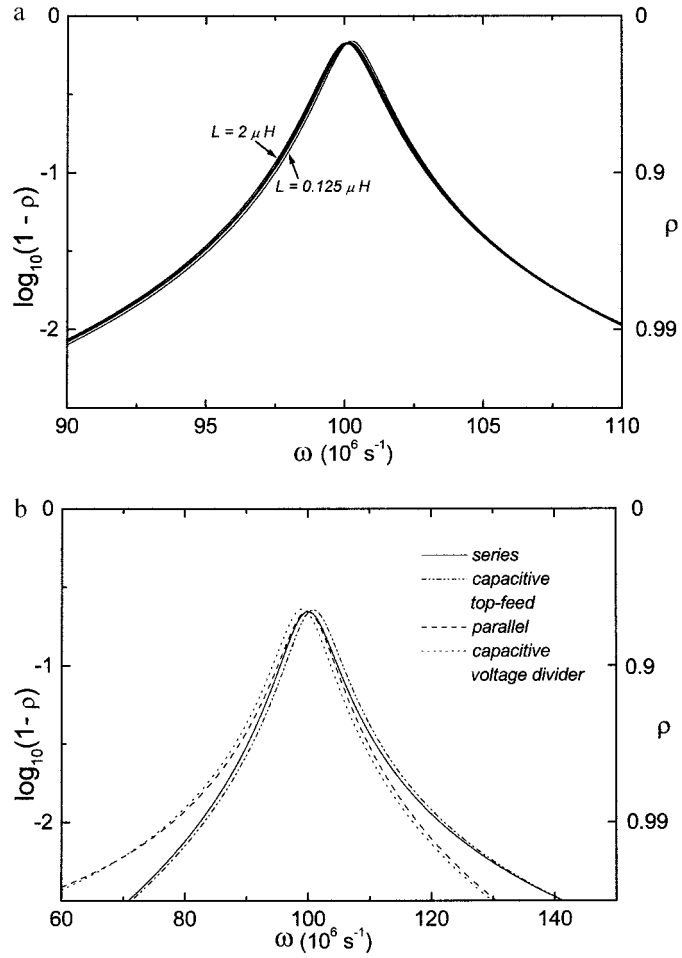


**FIG. 5.** (a) Comparison of reflection coefficients of tuned circuits of capacitive top-feed geometry of Fig. 1b. All circuits are $Q = 100$ and are adjusted to $EOC = 2$ (25 ohm real at $\omega_o$). Five values of $L$ are shown (0.125, 0.25, 0.5, 1, and 2 $\mu$H), with 5 corresponding values of the current division fraction, $C_2/(C_1 + C_2)$. (b) Comparison of the four tuned circuit geometries of Figs. 1a, 1b, 1c, and 1d. Each circuit has $EOC = 8$ with $Q = 100$. The results demonstrate that the tuning bandwidth is essentially the same for all tuned circuit geometries for a given extent of overcoupling ($EOC$).

Thus one is led to ask whether any of the geometries in Figs. 1a, 1b, 1c, or 1d has a broader tuning bandwidth than the others. Results for reflection coefficient $\rho$ are displayed in Fig. 5a for 5 tuned circuits, all of the capacitive top-feed arrangement of Fig. 1b. All have the same $Q = 100$ and are adjusted to give $R_{res} = 25$ ohms, corresponding to an overcoupling of $EOC = 2$. Five different values of $L$ are used, so that five different values of the current division fraction $C_2/(C_1 + C_2)$ are required. We note that while all five have the same $\omega_o$ describing the series resonance, the parallel resonances are at five different frequencies. The results in Fig. 5a indicate that all five circuits have essentially the same performance.

The four different geometries of Figs. 1a–1d are compared in Fig. 5b. Each circuit has $Q = 100$, $L = 0.5$ $\mu$H, $R_o = 50$ ohms, and overcoupling $EOC = 8$. Thus $R_{res}$ is 6.25 ohms for

the series-derived circuits (Figs. 1a and 1b) and 400 ohms for parallel-derived circuits (Figs. 1c and 1d). The results show only small shifts in center frequency, with essentially no differences in the tuning bandwidths. Similar results occur for other values of $EOC$, confirming the above conclusion. The shifts in center frequency become larger for larger values of $EOC$. In terms of remote tuning bandwidth, there is no reason to prefer any one tuned circuit geometry over others.

## III. CONCLUSIONS

NMR probe-tuned circuits may be approximately fixed-tuned near the rf coil and remotely tuned (or remotely fine-tuned) using a variable matching network on the end of a transmission line. Such an approach may be useful whenever it is inconvenient to locate variable tuning components near the NMR coil, such as in low-temperature or high-temperature NMR or in diamond anvil cell NMR. Also, the remotely located variable elements may have higher voltage and power ratings than variable components small enough to fit near the probe coil. The tuning bandwidth of such schemes is the frequency range over which the transmission line losses remain acceptably low.

The analysis of such circuits yields the following conclusions: (i) The tuning bandwidth may be much larger than the tuned circuit's natural bandwidth of $f_o/Q$, particularly if the transmission line has low loss (i.e., small matched-loss). (ii) Not surprisingly, the tuning bandwidth scales as $1/Q$. Thus, obtaining adequate tuning bandwidth is only an issue for high-$Q$ probe circuits. (iii) The key factors in obtaining a wide tuning bandwidth are the extent to which the transmission line is overcoupled to the probe tuned circuit and the matched-loss of the transmission line. (iv) For equivalent extents of overcoupling of the tuned circuit to the line, all geometries of tuned circuit (series, parallel, parallel with capacitive voltage division, and series with current division) yield essentially the same performance and tuning bandwidth.

## ACKNOWLEDGMENTS

The authors appreciate many conversations with R. A. McKay. We are most grateful for the helpful remarks of an anonymous referee. This work was supported in part by NSF Grant DMR 9705080.

## REFERENCES

1. E. Fukushima and S. B. W. Roeder, "Experimental Pulse NMR, A Nuts and Bolts Approach," Addison–Wesley, Reading, MA, 1981.
2. D. E. MacLaughlin, *Rev. Sci. Instrum.* **60,** 3242–3248 (1989).
3. D. I. Hoult and R. E. Richards, *J. Magn. Reson.* **24,** 71–85 (1976).
4. P. L. Kuhns, S.-H. Lee, C. Coretsopoulos, P. C. Hammel, O. Gonen, and J. S. Waugh, *Rev. Sci. Instrum.* **62,** 2159–2162 (1991).
5. A. P. Reyes, H. N. Bachmann, and W. P. Halperin, *Rev. Sci. Instrum.* **68,** 2132–2137 (1997).
6. O. Kanert, private communication.
7. H. Kolem, O. Kanert, H. Schulz, and B. Guenther, *J. Magn. Reson.* **87,** 160–165 (1990).
8. P. L. Kuhns and M. S. Conradi, *J. Magn. Reson.* **78,** 69–76 (1988).
9. W. Froncisz, A. Jesmanowicz, and J. S. Hyde, *J. Magn. Reson.* **66,** 135–143 (1986).
10. J. H. Walton and M. S. Conradi, *J. Magn. Reson.* **81,** 623–627 (1989).
11. A. R. Rath, *Magn. Reson. Med.* **13,** 370–377 (1990).
12. F. E. Terman, "Radio Engineer's Handbook," McGraw–Hill, New York, 1943.
13. R. W. P. King, H. R. Mimno, and A. H. Wing, "Transmission Lines, Antennas, and Wave Guides," McGraw–Hill, New York, 1945.
14. C. L. Hutchinson and J. P. Kleinman (Eds.), "The ARRL Handbook for Radio Amateurs," 1992 ed., American Radio Relay League, Newington, CT, 1992.
15. M. G. Pravica and I. F. Silvera, *Rev. Sci. Instrum.* **69,** 479–484 (1998).
16. M. S. Conradi, *Concepts Magn. Reson.* **5,** 243–262 (1993).
17. R. A. McKay, U.S. Patent 4,446,431, 01 May 1984, "Double-Tuned Single Coil Probe for Nuclear Magnetic Resonance Spectrometer."
18. Y. W. Kim, W. L. Earl, and R. E. Norberg, *J. Magn. Reson. A* **116,** 139–144 (1995).
19. J. A. Stringer and G. P. Drobny, *Rev. Sci. Instrum.* **69,** 3384–3391 (1998).